INTERNATIONAL JOURNAL OF OPTIMIZATION IN CIVIL ENGINEERING
Int. J. Optim. Civil Eng., 2020; 10(1):137-154

RELIABILITY BASED OPTIMIZATION OF 3D STEEL MOMENT FRAMES CONSIDERING AXIAL FORCE AND BIAXIAL BENDING MOMENTS INTERACTION

H.R. Irani[1], V.R. Kalatjari[1*, †] and M.H. Dibaei Bonab[2]
[1]*Civil Engineering Department, Shahrood University of Technology, Shahrood, Iran*
[2]*Faculty of Engineering, Islamic Azad University Shahrood Branch, Shahrood, Iran*

ABSTRACT

This paper presents a design process using a course grained parallel genetic algorithm to optimize three-dimensional steel moment frames by considering the axial force and biaxial bending moments interaction in plastic hinge formation. The objective function is to minimize the total weight of the structure subjected to the reliability constraint of the structural system. System reliability analysis is performed through the proposed Modified Latin Hypercube Simulation (M-LHS) Method. For optimization, a 3DSMF-RBO program is written in CSHARP programming language. The reliability analysis results show a large decrease in the number of simulation samples and subsequently a decrease in the execution time of optimization computation. The optimization results indicate that by considering interaction of the axial force and biaxial bending moments in plastic hinge formation rather than the only bending moment, to some extent increases the total weight of the designed structure.

Keywords: system reliability analysis; size optimization; 3D steel moment frame; parallel genetic algorithm; modified Latin hypercub.

Received: 12 October 2019; Accepted: 23 December 2019

1. INTRODUCTION

In the field of civil engineering one try to achieve specific objectives in order to optimize weight, cost of construction, geometry, layout, topology and computational time satisfying specific constraints. Since resources and time are always limited, solutions must be found to optimize the use of these resources [1, 2].

---

[*]Corresponding author: Civil Engineering Department, Shahrood University of Technology, Shahrood, Iran
[†]E-mail address: V_Kalatjari@shahroodut.ac.ir (V.R. Kalatjari)

The optimization of structural frames has been studied by considering stress and displacement constraints under different load combinations, which are usually applied to two formulations. The first uses mathematical programming and the second uses random search methods. Genetic algorithms (GA) are one of the most popular methods among the second group [3-5]. The main difference between the mentioned methods is that in mathematical programming it is necessary to calculate the objective function gradients whereas, in the second group, the global optimization is performed by random search without using the gradients [6].

Ignoring the probabilistic nature of the structural parameters with high uncertainty results in the structural response to the loads becoming erroneous and far from reality. Using the theory of structural reliability, these uncertainties can be established into mathematical relationships, and the safety and performance considerations of the structure can be quantitatively incorporated into the design process [7].

Generally, limit states or load and resistance factor design (LRFD) codes for building structures such as AISC [8] have been developed, taking into account the reliability of members of a structure individually. However, because of structural redundancy or redistribution of forces after the failure of a member, the failure of an individual member does not necessarily lead to the failure of the entire structural system. Therefore, evaluation of the reliability of a structural system is more important than the reliability of each structural member individually [9, 10].

Several methods have been proposed to determine the safety index or the probability of failure of the structural members, such as First order-Second moment [11], Hasofer-Lind [12] and Rakwitz-Fischler [13] methods. The Hasofer-Lind and Rackwitz-Fiessler methods are a high-precision matrix process based on iterations that can be difficult and time-consuming if the function is nonlinear and has a large number of variables. Therefore, in members such as columns in the moment frames under simultaneous axial force and biaxial bending moments, these methods will have their own problems due to the nonlinearity of the limit state function and the variety of random variables. Often for the sake of simplification, regardless of the simultaneous impact of axial force and biaxial bending moments, the failure criterion is considered due to the only bending moment failure [14, 15] or the effect of the axial force and bending moments separately [16].

When failure is defined as the creation of a mechanism in a structural system (collapse), determining the probability of failure requires identifying and analyzing a large number of significant failure mechanisms and that is time-consuming. Among the methods of estimating the probability of failure of the structural system, simulation techniques and methods based on the failure paths are the most common ones. In failure path-based methods, the most likely failure paths are first generated automatically, then the upper and lower bounds of the structural system failure are estimated based on these paths.

In simulation techniques, the loads and resistances of a structure are randomly simulated. The probability of failure is a ratio between the number of failure occurrence and the total number of simulations. The technique is easy to apply, but when the probability of failure is low, as is usually the case in real structural systems, the number of simulations will be high. So this method is not applicable to most real problems [17].

In the present study, the reliability-based optimization of three-dimensional steel moment frames by considering the axial force and biaxial bending moments interactions is investigated. The objective function is the weight of the structure so that the performance constraint is the overall probability failure of the structural system. The optimization is performed using a parallel genetic algorithm for which a program is written with CSHARP programming software. In the reliability analysis, uncertainties in loads, material properties, cross-section and plastic section modulus of members are taken into account. Reliability analysis has been performed using the proposed Modified Latin Hypercube simulation (M-LHS) method which results are in an acceptable accuracy in a shorter period of time. The methods and results of the analysis are described in the following sections.

2. FINITE ELEMENT ANALYSIS AND GENERATION OF SAFETY MARGINS

Consider an arbitrary member of a space frame as shown in Fig. 1. In the local coordinate system of the member, the displacements of the end members by u1 to u12 and the corresponding end forces by Q1 to Q12 are shown.

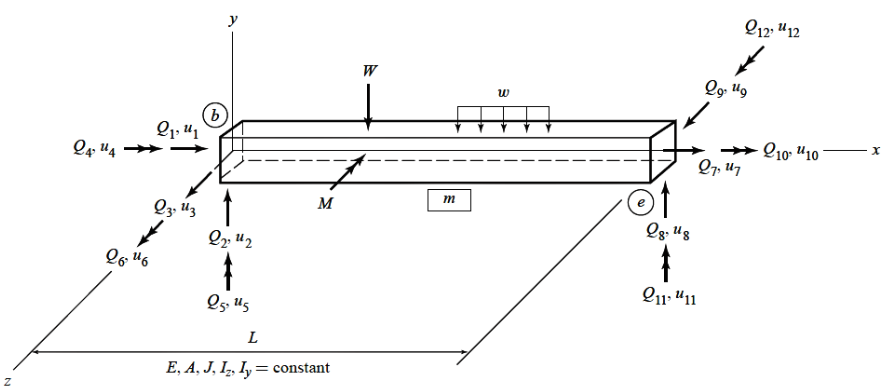

Figure 1. Member forces and displacements in the local coordinate system

when the member is in the elastic range, the relationship between the end forces Q_t and the end displacements u_t can be expressed as follows:

$$\overline{Q}_t = \overline{\overline{k}}_t \overline{u}_t \tag{1}$$

where $\overline{\overline{k}}_t$ is the local stiffness matrix of the space frame members by arranging all the stiffness coefficients in a 12 × 12 matrix. After a section of the member has yielded, i.e. the plasticity condition $F_k = 0$ (k= i, j) is obtained, the relation between Q_t and u_t will be derived as in the following:

$$\overline{Q}_t^{(p)} + \left(-\overline{Q'}_t^{(p)}\right) = \overline{\overline{k}}_t^{(p)} \overline{u}_t \tag{2}$$

where $\overline{\overline{k}}_t^{(p)}$ is the reduced stiffness matrix of the member and $\overline{Q'}_t^{(p)}$ is the opposite sign of the equivalent nodal force vector that is given in equations 10 to 13.

When each end of the member is failed, redistribution of the internal forces is performed at the end of the members, after which the analysis is re-performed and the subsequent failure is determined. The stiffness matrix of the failed member is modified and the equivalent nodal forces are applied to the nodes. After the same process is repeated, a structural failure occurs when a specified number of member ends are damaged. Mechanism formation is determined by investigating the singularity of the total reduced stiffness matrix of the structure $\overline{\overline{K}}^{(p_q)}$. The criterion for structural failure is given by [18]:

$$\left| \overline{\overline{K}}^{(p_q)} \right| = 0 \tag{3}$$

where | • | is the determinant of a matrix and superscript P_q denotes the P_q^{th} failure stage.

2.1 Generation of safety margins for frame structures subjected to the single load effect

Consider a structural frame with *n* members. As the applied bending moments extend beyond the fully plastic capacity, the members are assumed to fail and plastic hinges are formed. In structural frames, it is assumed that the plastic hinges are formed at the member ends. The safety margins of the member ends are [18]:

$$M_i = R_i - S_i \qquad (i = 1,2,....,2n) \tag{4}$$

where R_i are the strengths of the member ends defined by the full plastic moment capacity of the members (i.e. $R_i=Z_{pi}.F_{yi}$) and S_i are the bending moments at the end of the members. As a result, the criterion for end-member failure is given by:

$$M_i \leq 0 \tag{5}$$

when a plastic hinge is formed at the left or right end of a member or when formed at both ends of the member, as stated in Section 5.3 of Ref. [18] and Section 8.3 of Ref. [19], the stiffness matrix of the member is replaced by a reduced matrix $\overline{\overline{k}}_t^{L}$, $\overline{\overline{k}}_t^{R}$ or $\overline{\overline{k}}_t^{RL}$ respectively, and the equivalent nodal forces $\overline{Q'}_t^{L}$, $\overline{Q'}_t^{R}$ or $\overline{Q'}_t^{RL}$ are applied to the ends of the members.

2.2 Generation of safety margins for frame structures subjected to the combined load effect

In order to consider the interaction effect of internal forces on plasticized conditions, the yield function with a linear surface is approximated according to Equation 8.

$$F_k = R_k - \overline{C}_k^T \overline{Q}_t = 0 \qquad (k = i, j) \tag{8}$$

where R_k is the strength of the member end k, and the vector $\overline{C}_k^T$ is determined by the dimension of the member. In Space frames, when the plastic moment capacity about the z-axis is taken as the reference strength, R_k and $\overline{C}_k^T$ are given by:

$$\begin{aligned} R_k &= F_{yk}.Z_{z_{pk}} \\ \overline{C}_i &= \left(\frac{Z_{z_{pi}}}{A_{pi}} Sign(F_{xi}),0,0,0,\frac{Z_{z_{pi}}}{Z_{y_{pi}}} Sign(M_{yi}), Sign(M_{zi}),0,0,0,0,0,0 \right) \\ \overline{C}_j &= \left(0,0,0,0,0,0,\frac{Z_{z_{pj}}}{A_{pj}} Sign(F_{xj}),0,0,0,\frac{Z_{z_{pj}}}{Z_{yj}} Sign(M_{yj}), Sign(M_{zj}) \right) \end{aligned} \tag{9}$$

where A_{pi} and A_{pj} are cross-sectional areas, $Z_{z_{pk}}$ and $Z_{y_{pk}}$ are the plastic section modulus about the z and y axes, respectively. Using equation (2), the explicit form of $\overline{\overline{k}}_t^{(p)}$ and $\overline{Q'}_t^{(p)}$ will be as follows [18]:

1) Where the member is elastic:

$$\left. \begin{aligned} \overline{\overline{k}}_t^{(p)} &= \overline{\overline{k}}_t \\ \overline{Q'}_t^{(p)} &= \overline{0} \end{aligned} \right\} \tag{10}$$

2) In case of failure at the left-hand end:

$$\left. \begin{aligned} \overline{\overline{k}}_t^{(p)} (= \overline{\overline{k}}_t^L) &= \overline{\overline{k}}_t - \overline{\overline{k}}_t \overline{C}_i^T \overline{C}_i \overline{\overline{k}}_t \Big/ (\overline{C}_i \overline{\overline{k}}_t \overline{C}_i^T) \\ \overline{Q'}_t^{(p)} (= \overline{Q'}_t^L) &= R_i \overline{\overline{k}}_t \overline{C}_i^T \Big/ (\overline{C}_i \overline{\overline{k}}_t \overline{C}_i^T) \end{aligned} \right\} \tag{11}$$

3) In case of failure at the right-hand end:

$$\left. \begin{aligned} \overline{\overline{k}}_t^{(p)} (= \overline{\overline{k}}_t^R) &= \overline{\overline{k}}_t - \overline{\overline{k}}_t \overline{C}_j^T \overline{C}_j \overline{\overline{k}}_t \Big/ (\overline{C}_j \overline{\overline{k}}_t \overline{C}_j^T) \\ \overline{Q'}_t^{(p)} (= \overline{Q'}_t^R) &= R_j \overline{\overline{k}}_t \overline{C}_j^T \Big/ (\overline{C}_j \overline{\overline{k}}_t \overline{C}_j^T) \end{aligned} \right\} \tag{12}$$

4) In case of failure at both ends of member:

$$\left.\begin{aligned} &\overline{\overline{k}}_t^{(p)} (= \overline{\overline{k}}_t^{LR}) = \overline{\overline{k}}_t - \overline{\overline{H}}^T \overline{\overline{G}}^{-1} \overline{\overline{H}} \\ &\overline{Q'}_t^{(p)} (= \overline{Q'}_t^{LR}) = \overline{\overline{H}}^T \overline{\overline{G}}^{-1} \begin{Bmatrix} R_i \\ R_j \end{Bmatrix} \end{aligned}\right\} \tag{15}$$

where

$$\overline{\overline{G}}^{-1} = \begin{bmatrix} \overline{C}_i \overline{\overline{k}}_t \overline{C}_i^T & \overline{C}_i \overline{\overline{k}}_t \overline{C}_j^T \\ \overline{C}_j \overline{\overline{k}}_t \overline{C}_i^T & \overline{C}_j \overline{\overline{k}}_t \overline{C}_j^T \end{bmatrix}^{-1} \qquad \overline{\overline{H}} = \begin{bmatrix} \overline{C}_i \overline{\overline{k}}_t \\ \overline{C}_j \overline{\overline{k}}_t \end{bmatrix}$$

3. SYSTEM RELIABILITY EVALUATION

The reliability of a structure is usually measured by probability values such as probability of failure Pf, and reliability index β. Fig. 2 schematically illustrates the problem of structural member reliability. On the left side of the figure, there are two probability density functions for "load effects" and "resistance". As long as the resistance R is greater than the load effects S, R>S, the member is safe. On the right side of the figure, a combined PDF for the safety margin called the reliability function (g = R - S) is shown. If the value of this function is positive, the member will resist loads. If the value is negative, a failure occurs. The probability of failure (defined as $0 \le Pf \le 1.0$) is indicated by the solid area on the left of the Y-axis [20].

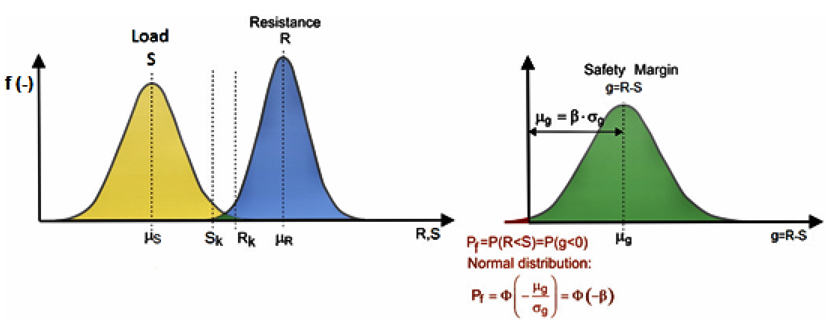

Figure 2. Representation of the structural member reliability problem [20]

The structure failure probability, Pf, is given by the following formula:

$$p_f = J = \int_{G(X)\le 0} f_X(x)dx \tag{14}$$

where $X=[x_1, x_2, \ldots, x_n]^T$ is a vector of random variables of the reliability problem, and $f_X(x)$ refers to a joint probability density function in X-space. The performance of each structure can be expressed by the limit state function of the random variables of that structure, with *G(X)>0* indicating a safe state and *G(X)<0* failing. Evaluation of this multiple probability integral is a fundamental problem in structural reliability theory. The direct calculation of this integral is difficult, especially for real structures [21-23].

3.1 Monte carlo simulation

In the Monte Carlo method, an estimate of the probability of failure is presented by the following relation [24]:

$$\overline{p}_f = \frac{1}{N}\sum_{i=1}^{N} I(X_1, X_2, \ldots\ldots, X_n) \tag{15}$$

where $I(X_1, X_2, \ldots, X_n)$ is a function defined as follows:

$$I(X_1, X_2, \ldots\ldots, X_n) = \begin{cases} 1 & if \quad G(X_1, X_2, \ldots\ldots, X_n) \le 0 \\ 0 & if \quad G(X_1, X_2, \ldots\ldots, X_n) > 0 \end{cases} \tag{16}$$

According to relation 16, *N* independent sets of values $x_1, x_2, \ldots, x_n$ are obtained on the basis of the probability distribution for each random variable and the failure function is computed for each sample. Using MCS, an estimate of the probability of structural failure is obtained as follows:

$$\overline{p}_f = \frac{N_H}{N} \tag{17}$$

where N_H is the total number of cases where failure has occurred ($\left|\overline{\overline{K}}^{(p)}\right| \le \varepsilon$).

3.2 Modified-latin hypercube sampling

In order to reduce the statistical error in MSC, the number of samples must be very large and therefore the number of calculations will be high. For this reason, various sampling techniques have been developed to reduce the sample size and improve the accuracy of the prediction. These include important sampling, adaptive sampling technique, Latin hypercube sampling and conditional expectation technique. Latin Hypercube Sampling (LHS) is generally recognized as one of the most efficient techniques of size reduction.

In the LHS sampling method, the sampling space is divided into strata and only a few of the many possible samples per interval are selected. Finally, there are N sets of samples that can be interpreted as N vectors, selected in the Monte Carlo simulation technique and used directly in Eq. (17), Ref. [25].

In the LHS technique, strata can be fixed or variable. In order to reduce the number of simulations in the present study, a specific variable interval is proposed called Modified Latin Hypercube Sampling (M-LHS). In the M-LHS technique, the arrangement of the intervals according to Fig. 3 is such that at the $+\sigma_x \pm \sigma_x/2$ and $-\sigma_x \pm \sigma_x/2$ (σ_x is the standard deviation of random variable X) distance of the mean value, we have the highest density of selected variables. Based on the solved examples, it is suggested that approximately 75% of the variable simulation be selected from these ranges. It should be noted that the proposed method is applicable to design variables with Normal, Log-Normal, Extreme Type I and Extreme Type II PDFs and requires further review for other PDFs.

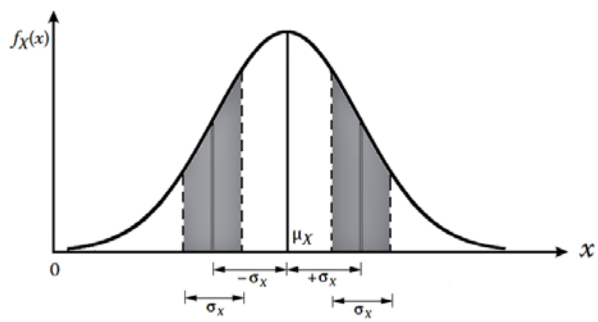

Figure 3. Arrangement of strata in M-LHS technique

4. RELIABILITY-BASED STRUCTURAL OPTIMIZATION

In the present study, the reliability-based optimization of multi-story 3D steel moment frames has been investigated. In deterministic sizing optimization problems, the objective is to minimize the weight of the structure under certain deterministic constraints such as stresses and displacements. In optimal reliability-based design, additional probabilistic constraints are applied to allow different random parameters and the probability of structural failure to be within the acceptable ranges (e.g. 10^{-3}). In this study, the probability of structural system failure, as a result of a limit Elasto-plastic analysis, is considered as the global reliability constraint.

Consider a steel structure of N_m members defined in the N_d design groups. In the optimal design programming problem, you need to find a vector of integer values **I** (Eq. 18) that represent the number of steel sections assigned to N_d member groups.

$$\mathbf{I}^{\mathrm{T}} = \lfloor I_1, I_2, ..., I_{N_d} \rfloor \tag{18}$$

The aim is to minimize the weight (W) of the structural frame:

$$W = \sum_{i=1}^{N_d} \rho_i A_i \sum_{j=1}^{N_t} L_j \tag{19}$$

So that the following condition is not violated.

$$P_{f_S} \le P_{f_{\max}}^{System} \tag{20}$$

In the above equations, A_i and ρ_i are the cross-sectional area and unit weight of the steel section adopted for members of group *i*, respectively, N_t is the number of members in group *i*, and L_j is the length of the member *j* of group *i*. $P_{f\,\mathrm{S}}$ is the probability failure of the structural system and $P_{f\,\max}^{\,System}$ indicates the maximum allowable value of the structural failure probability.

4.1 Genetic algorithm

The main feature of GA is the survival of the best. GA starts with an initial population of randomly generated individuals. Each individual (*chromosome*) has some structural data that represents a possible solution in the problem search space.

GA consists of three main parts: 1) encoding and decoding variables into strings 2) evaluating the fitness of each solution, and 3) applying genetic operators (selection, intersection and mutation) to generate the next generation. By evaluating each individual's fitness, the value of the objective function will be penalized if the limitations are violated. This process is repeated until a termination condition is satisfied.

4.2 Multi search method

The multi search method divides the entire population into sub-populations (Islands) and implements a GA standard for each. Before producing the next generation, the information (the best individuals) is exchanged between the sub-populations. In the parallelization process, it is important to know the migration interval and the migration rate.

The migration operator randomly sends a percentage of the best of one subpopulation to another island, which has a different structure of environment and members (Figure 4). After the migration process, the genetic algorithm combines the populations of immigrants with the rest of the population and moves towards a more fit population. Because the characteristics of the space of each island are distinct, the answers vary greatly during the search process. As such, each optimization problem is examined and searched in an instant with several methods and then the best results are shared between the other islands. These properties collectively reduce the influence of parameters and relationships governing GA operations and increase the convergence speed of the algorithm [26].

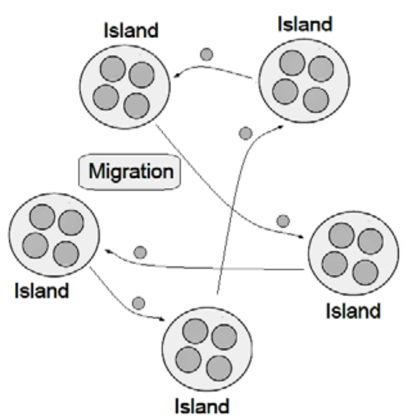

Figure 4. Multi search method through random migration

To select the appropriate chromosomes, a combination of tournament selection, random selection and roulette wheel methods has been used in the islands. Also, using the elitist strategy, some of the fittest current-generation chromosomes are transferred directly to the next generation. The crossover operation also uses uniform, single-point and double-point crossover methods. A linearly decreasing mutation rate is also used in the mutation operation.

5. FEATURES OF THE CODE WRITTEN FOR OPTIMIZATION OF THE 3D STEEL MOMENT FRAMES

A code named *3DSMF-RBO* has been written to optimize the reliability of the three-dimensional steel moment frame by considering the axial force and biaxial bending moments interaction. Solutions are also provided to reduce the time required for the process of reliability analysis and optimization.

In calculating the probability of structural failure, using the M-LHS method significantly reduces the computational time, which the next section presents the validation of this method. In Genetic Algorithms, one of the simplest solutions is that all non-duplicate chromosomes that have not been produced in previous generations with the values of the objective function and the penalty function are stored in a set called "NonDup". After the second generation, if a chromosome resembles duplicated chromosomes, it will not be evaluated and existing results are used directly [27].

6. CASE STUDIES

The solutions algorithms presented in the previous sections are computerized in a design and optimization software that is compiled in *CSHARP* source code.

To evaluate the performance of the written program, an M-LHS technique verification was first performed on two 3-storey and 6-storey structures. Then, to investigate the performance of 3DSMF-RBO program, two examples of two-dimensional and three-dimensional steel moment frames are considered, the results of which are presented in the next section.

6.1 Example 1: Evaluation of M-LHS method

First, the validation of the written program to calculate the probability of failure by the Monte Carlo method is discussed. For this purpose, two frames are selected as examples from references [30] and [31]. The reference frame [30] is a two-dimensional two-storey, two-span frame with gravity and lateral point loads that its probability of failure is obtained with 5000 simulations. The reference frame [31] is a two-storey, single-span frame with uniform gravity loads and concentrated lateral loads whose probability of failure is calculated by 20,000 simulations. The results of the frame failure probability in the above references and the probability of failure of the written program are presented in Table 1.

Table 1. Verification results of failure probability for Monte-Carlo analysis

	Reference Frame [30]	Reference Frame [31]
Probability Failure of References	$P_f = 0.116$	$P_f = 0.00175$
Probability Failure by Written Program	$P_f = 0.12$	$P_f = 0.00173$

In order to validate the M-LHS method, two three-story and six-story 3D steel frames are provided in accordance with Fig. 5. The design of these frames are based on the American Steel Structures Design and Loading Regulations [8, 32] using ETABS software that the geometric properties of the frame members are shown in Table 2.

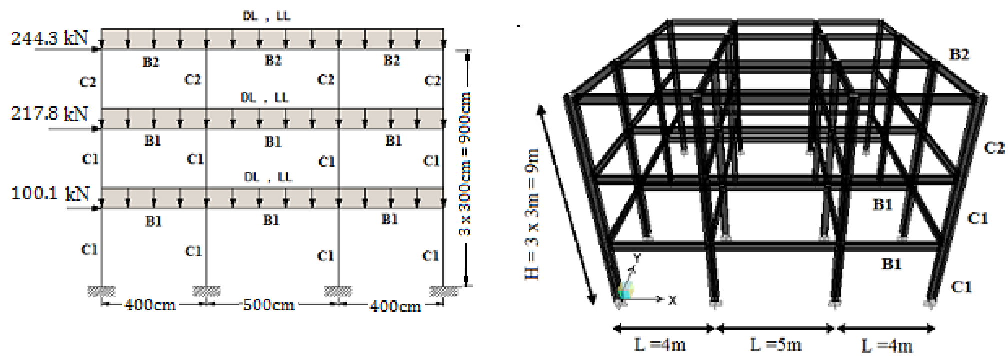

a) Three-story steel moment frame

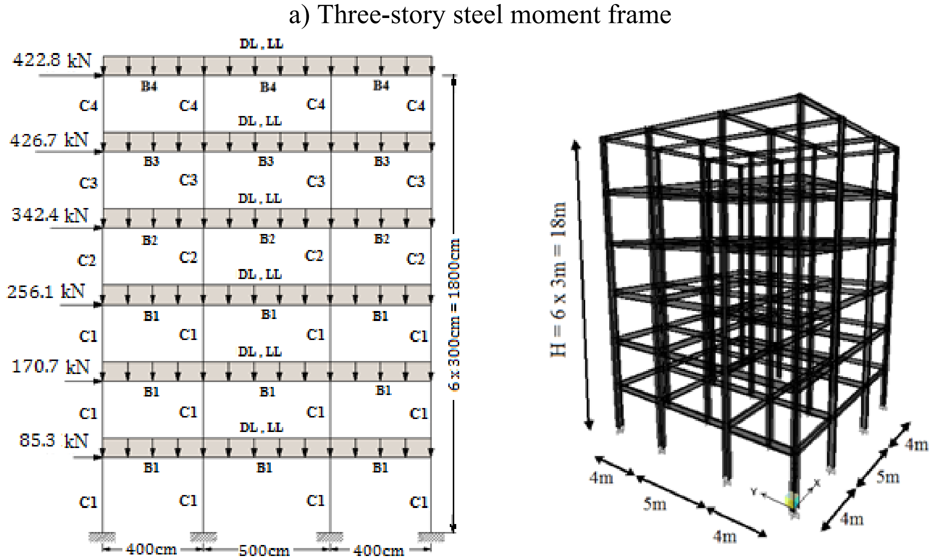

b) Six-story steel moment frame

Figure 5. Three-dimensional steel moment frames

Table 2: Section properties of frame members
(a) Three-story frame

Story	Member	Profile	Cross Sectional Area (cm^2)	Plastic Section Modulus about Z Axis (cm^3)	Plastic Section Modulus about Y Axis (cm^3)
1 , 2	**C1**	HE 240B	106	1053	498
	B1	IPE 300	53.8	628	125
3	**C2**	HE 220B	91	827	394
	B2	IPE 240	39.1	367	73.9

(b) Six-story frame

Story	Member	Profile	Cross Sectional Area (cm^2)	Plastic Section Modulus about Z Axis (cm^3)	Plastic Section Modulus about Y Axis (cm^3)
1 , 2 , 3	C1	HE 360B	181	2683	1032
	B1	IPE 360	72.7	1019	191
4	C2	HE 340B	171	2408	986
	B2	IPE 330	62.6	804	154
5	C3	HE 280B	131	1534	718
	B3	IPE 300	53.8	628	125
6	C4	HE 240B	106	1053	498
	B4	IPE 240	39.1	367	73.9

The probabilistic properties of all random variables are given in Table 3.

Table 3: Properties of random variables

Random Variable	PDF	Nominal Value	Bias Factor ($\lambda = \frac{Mean}{Nominal}$)	Coefficient of Variation (C.O.V)	Reference
Yield Stress F_y	Log-N	2400 *Kgf/cm^2*	1.1	0.1	[33] Hess et al, 2011
Dead Load *D*	N	Variable	1.05	0.1	[34] Ellingwood et al, 1982
Live Load *L*	Extreme Type I	Variable	1.0	0.15	[11] Nowak, 2010
A and Z	Log-N	Variable	1.04	0.05	[33] Hess et al, 2002
Earthquake *E*	Extreme Type II	$\frac{Mean}{V} = 0.659$	$\alpha = 3.3$	0.56	[35] Ellingwood et al, 1996

The results of these analyzes with 100'000 Monte Carlo simulations, 5000 LHS simulation with uniform intervals and 1000 M-LHS simulations are presented in Table 4.

Table 4. Monte-Carlo, LHS and M-LHS method Results

		Reliability Index β	**Failure Probability P_f**
3- Story Moment Frame	MC Method	3.06	$1.12x10^{-3}$
	LHS Method	3.09	$1.0x10^{-3}$
	M-LHS Method	3.09	$1.0x10^{-3}$
6- Story Moment Frame	MC Method	3.03	$1.23x10^{-3}$
	LHS Method	3.09	$1.0x10^{-3}$
	M-LHS Method	3.09	$1.0x10^{-3}$

As can be seen, the selection of 75% of the samples in the range defined in section 3.2, reduces the number of simulated samples for each variable from 100,000 samples in the Monte Carlo simulation method to 1000 samples in the M-LHS method. As a result, it will have a significant impact on the execution time of the computational probability of structural system failure and finally on the performance of optimization calculations.

6.2 Example 2: Optimization of one-bay eight-story frame

As shown in Fig. 6 an eight-story two-dimensional structural frame is considered for optimal design. This structure has been optimized by Khot et al. using the optimality criterion method [36]. According to Fig. 6, 24 structural members are classified into eight groups. An 8-digit binary number is used to represent 268 W-sections of the AISC. The only constraint is that the lateral drift at the top of the structure is not more than 2 inches.

For algorithm convergence, the algorithm requires an average of approximately 30 generations. The results are compared with those of [36, 37] as presented in Table 5.

Table 5: Comparison of the results for one-bay, eight-story frame

Group number	**Number of members**	**Khot et al. [36]**	**Kaveh et al. [37]**	**Present work**
1	4	W14×34	W21×44	W18×35
2	4	W10×39	*W*18×35	W16×31
3	4	W10×33	*W*14×22	W14×30
4	4	W8×18	*W*12×14	W10×15
5	2	*W*21×68	W16×26	W18×35
6	2	*W*24×55	*W*18×40	W21×44
7	2	W21×50	*W*18×35	W18×35
8	2	W12×40	W12×22	W14×22
Total weight [kN(kips)]	-	41.02 (9.22)	31.38 (7.051)	31.86(7.16)

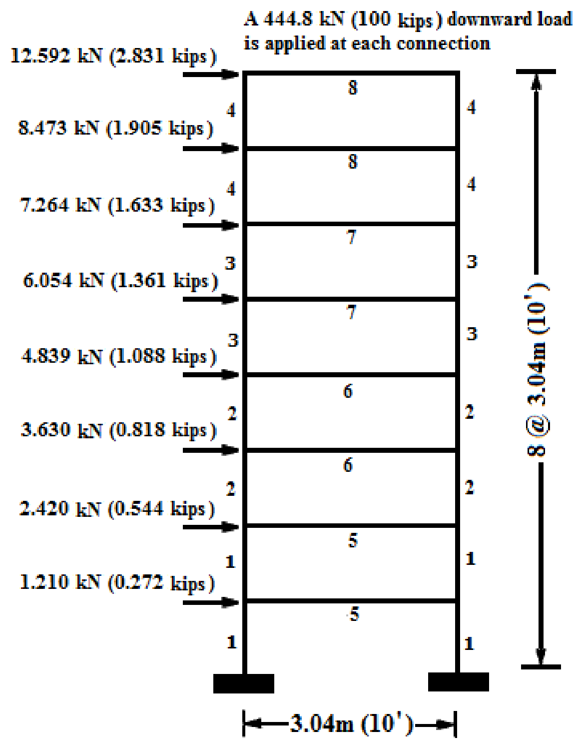

Figure 6. A one-bay, eight-story moment frame structure

6.3 Example 3: Optimization of 6-story 3D steel moment frame

The steel moment frame shown in Fig. 5b is selected as the third example to evaluate the performance of the written search algorithm. As can be seen in Fig. 7, 192 frame members are collected into 15 groups so that the columns and beams are identical in two adjacent stories. 268 sections of the W-section are used to assign members. The frame is subjected to a 1.0G + 1.0E combination of gravity (dead and live) loads and lateral (earthquake) loads. Earthquake loads are obtained as equivalent lateral forces outlined in the ASCE-2017 [32] that apply as point loads on the exterior nodes of each respective story (Fig. 5b). Table 6 shows the gravity loading applied to the beams of the roof and floors. The probabilistic properties of all random variables are as in Example 1.

Table 6: Gravity loading on beams of 6-story 3D steel moment frame

Story	**Uniformly distributed load (kN/m)**	
	Outer beams	**Inner beams**
Roof	9.42	14.91
Floor	14.7	17.66

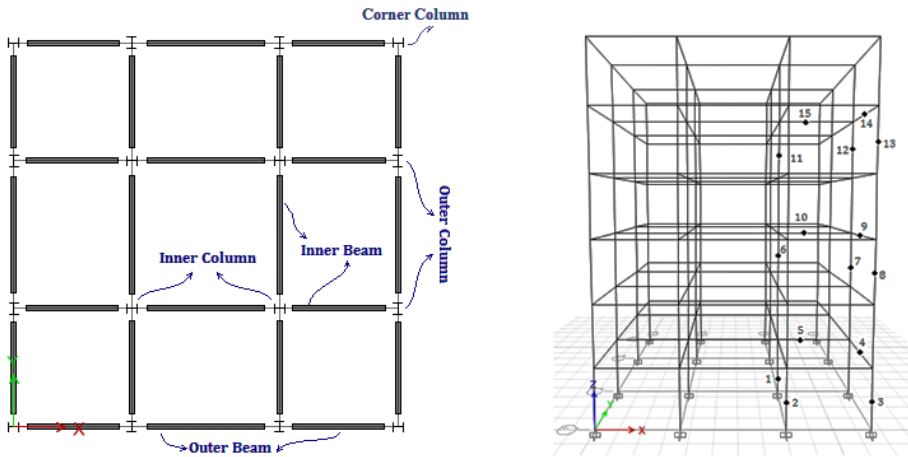

a) Plan view b) 3D view

Figure 7. Member groups of 6-story 3D steel moment frame

The performance constraint is the probability failure of the structural system ($P_{f\ system}$ no more than 1.0×10^{-3}). Frame optimization is accomplished by using a "coarse-grained parallel strategy" by generating 100 initial-population that are equally distributed in five sub-populations. The migration intervals are in the 20th generation, with 5 percent of chromosomes migrating.

In order to investigate the effect of axial force and biaxial bending moments interaction on frame optimization, frame analysis and optimal design have been performed twice. In the first case, the effect of axial force is neglected using the relations of Section 2.1 and in the second case, the axial force and biaxial bending moments interactions are considered using Section 2.2 relations.

The final design and cross-sections obtained for 15 member groups through the *3DSMF-RBO* search program are listed in Table 7. Moreover, the design history curve is shown in Fig. 8. As shown in Fig. 8, the 3DSMF-RBO program reduces the total weight of the structure in which interaction between axial force and bending moment is considered, from 2115.4 kN to 573.77 kN in approximately 200 non-ascending generations. As can be seen, there are few changes to the optimal design of the structure after the 100^{th} generation.

According to the results of Table 7, it can be seen that considering the interaction of axial force and biaxial bending moments, the sections of some columns have changed and the optimum weight of the designed structure has increased by about 4%.

Table 7: The optimum design of 6-story 3D steel moment frame

Group number	**Type of elements**	**Number of members**	**Designation with P-M interaction**	**Designation without P-M interaction**
1	Inner column	8	W14×90	W16×89
2	Outer column	16	W16×89	W16×77
3	Corner column	8	W16×67	W16×67
4	Outer beam	24	W16×26	W16×26
5	Inner beam	24	W16×31	W16×31

6	Inner column	8	W12×72	W12×72
7	Outer column	16	W12×79	W12×72
8	Corner column	8	W12×53	W12×53
9	Outer beam	24	W16×31	W16×31
10	Inner beam	24	W16×36	W16×36
11	Inner column	8	W10×49	W10×45
12	Outer column	16	W12×65	W12×58
13	Corner column	8	W8×31	W8×31
14	Outer beam	24	W10×30	W10×30
15	Inner beam	24	W10×26	W10×26
Total weight (kN)	-	-	573.77	553.61

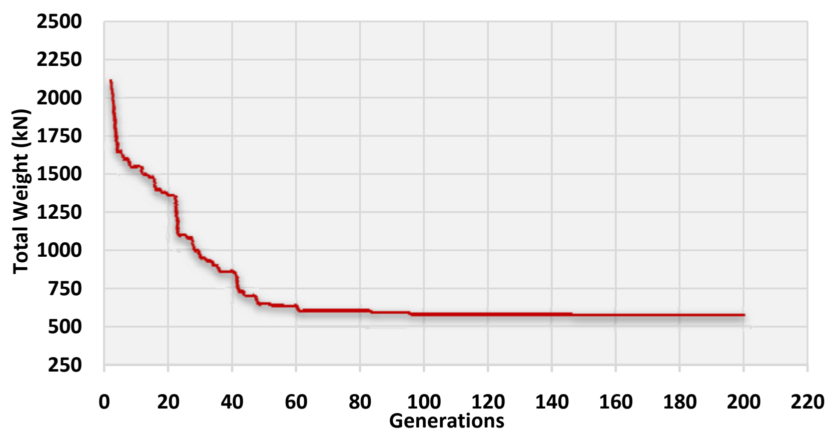

Figure 8. The design history graph obtained for 6-story 3D steel moment frame in which interaction between axial force and biaxial bending moments is considered

7. CONCLUSION

A computer program called 3DSMF-RBO to optimize the size of moment frame structures under reliability constraint by considering the axial force and biaxial bending moments interaction of elements is developed in this paper.

In order to calculate the probability of structural system failure, a modified hypercube simulation method, M-LHS, was proposed and investigated. For this purpose, the reliability analysis of a 3-storey moment frame and a 6-storey moment frame was performed using the Monte Carlo simulation and M-LHS method. It was observed that by reducing the number of simulated samples for each random variable from 100`000 samples in the Monte Carlo method and 5000 samples in LHS method to 1000 samples in the M-LHS method, the failure probability results were well approximated. Therefore, the time of performing the structural failure probability calculation and finally the execution time of optimization calculation is significantly reduced.

In the developed 3DSMF-RBO program, the optimization is carried out using the parallel genetic algorithm and the performance constraint is the probability of structural system failure using the M-LHS method. The results of the design of a 6-storey 3D frame refer to the efficiency of the developed program. According to the design sections and weights obtained for the optimized example, it was observed that by considering the interaction of axial force and biaxial bending moments of members, the size of some columns was enlarged and the optimum weight increased somewhat.

REFERENCES

1. Kaveh A. *Advances in Metaheuristic Algorithms for Optimal Design of Structures*, Springer International Publishing, Switzerland, 2nd edition, 2017.
2. Kaveh A. *Applications of Metaheuristic Optimization Algorithms in Civil Engineering*, Springer, Switzerland, 2017
3. Holland JH. *Adaptation in Natural and Artificial Systems*, MIT Press, Cambridge, MA, 1992.
4. Goldberg DE. *Genetic Algorithms in Search*, Optimization and Machine Learning, Addison Wesley, MA, 1989.
5. Jenkins WM. Plane frame optimum design environment based on genetic algorithm, *J Struct Eng, ASCE* 1992; **118**(11): 3103–12.
6. Kaveh A, Kalatjari VR. Topology optimization of trusses using genetic algorithm, force method and graph theory, *Int J Numer Meth Eng* 2003; **58**(5): 771-91.
7. Kaveh A, Kalatjari VR. *Theory of Reliability and Its Application in the Structure*, University of Science and Technology, Tehran, Iran, 1995.
8. American Institute of Steel Construction, AISC, *Specification for Structural Steel Buildings*, Chicago, USA, 2016.
9. Zhou W, Hang HP. System and member reliability of steel frames, *J Steel Composite Struct* 2004; **4**(6): 419-35.
10. Ellingwood BR. LRFD: Implementing structural reliability in professional practice, *Eng Struct* 2000; **22**(2): 106-15.
11. Nowak AS, Collins KR. *Reliability of Structures*, Taylor and Francis Group, 2nd Edition, 2012.
12. Hasofer AM, Lind N. An exact and invariant first order reliability format, *J Eng Mech, ASCE* 1974; **100**: 111-21.
13. Rackwitz R, Fiessler B. Structural reliability under combined random load sequences, *Comput Struct* 1978; **9**: 489-94.
14. Rashed R, Moses F. Application of linear programing to structural system reliability, *Comput Struct* 1986; **24**: 375-84.
15. Ang AHS, Ma HF. On the reliability of structural systems, *3rd International Conference on Structural Safety and Reliability, Elsevier,* Amsterdam, 1981, pp. 295-314.
16. Ghasemi MR, Yousefi M. Reliability-based optimization of steel frame structures using modified genetic algorithm, *Asian J Civil Eng* 2011; **12**: 449-75.
17. Park S, Choi S, Sikorski C, Stubbs N. Efficient method for calculation of system reliability of a complex structure, *Int J Solid Struct* 2004; **41**: 5035-50.

18. Thoft-Christensen P, Murotsu Y. *Application of Structural Systems Reliability Theory*, Springer-Verlog, Heidelberg, Berlin, 1986.
19. Kassimali A. *Matrix Analysis of Structures*, Cengage Learning, 2nd Edition, Carbondale, 2012.
20. Taras A, Huemer S. On the influence of the load sequence on the structural reliability of steel members and frames, *J Struct* 2015; **4**: 91-104.
21. Kaveh A, Dadras A. An efficient method for reliability estimation using the combination of asymptotic sampling and weighted simulation, *Sci Iran* 2019; **26**(4): 2108-22.
22. Kaveh A, Ilchi-Ghazaan M. Structural reliability assessment utilizing four metaheuristic algorithms, *Int J Optim Civil Eng* 2015; **5**(2): 205-25.
23. Kaveh A, Massoudi MS, Ghanooni Bagha M. Structural reliability analysis using charged system search algorithm, *Iranian J Sci Technol* 2014; **38**(C2): 439-48.
24. Cardoso JB, Almeida JR, Dias JM, Coelho PG. Structural reliability analysis using Mont-Carlo simulation and neural networks, *Advanc Eng Softw* 2008; **39**: 505-13.
25. Melchers RE, Beck AT, *Structural Reliability Analysis and Prediction*, NJ: Wiley, 2nd Edition, Hoboken, 2018.
26. Kalatjari VR, Talebpour MH. Sizing and topology optimization of truss structures by modified multi search method, *J Civil Survey Eng* 2011; **45**(3): 351-63.
27. Kaveh A, Kalatjari VR, Mansoorian P. Fast reliability-based optimization using parallel genetic algorithm, developed force method and artificial intelligence, *J Civil Eng Ferdowsi* 2013; **24**(2): 1-26.
28. Talebpour MH, Kaveh A, Kalatjari VR. Optimization of skeletal structures using a hybridized ant colony-harmony search-genetic algorithm*, IJST, Transact Civil Eng* 2014; **38**(C1); 1-20.
29. Biabani-Hamedani K, Kalatjari VR. Structural system reliability-based optimization of truss structures using genetic algorithm, *Int J Optim Civil Eng* 2018; **8**(4):565-86.
30. Gorman MR, Moses F. *Reliability of Structural Systems*, Case Western Reserve University, Report No.79-2, 1972.
31. Hadianfard MA, Razani R. Effect of semi-rigid behavior of connections in the reliability of steel frames, *J Struct Safe* 2003; **25**: 123-38.
32. American Society of Civil Engineering, ASCE/SEI, *Minimum Design Loads and Associated Criteria for Buildings and Other Structures,* Virginia, USA, 2017.
33. Hess PE, Bruchman D, Assakkaf IA, Ayyub BM. Uncertainties in material and geometric strength and load variables*, Naval Eng J*, Technical Report, 2002; **114**: 139-66.
34. Ellingwood B, MacGregor JG, Galambos TV, Cornell CA. Probability based load criteria: load factors and load combinations, *J Struct Div*, *ASCE* 1982; **108**(515): 950-64.
35. Ellingwood B, Rosowsky D. Combining snow and earthquake load for limit state design, *J Struct Eng* 1996; **122**(11): 1364-8.
36. Khot NS, Venkayya VB, Berke L. Optimization of structures for strength and stability requirements, *Air Force Flight Dynamics LAB Wright-Patterson AFB*, Ohaio, 1973, No. AFFDLTR-73-98.
37. Kaveh A, Malakoutirad S. Hybrid genetic algorithm and particle swarm optimization for the force method-based simultaneous analysis and design, *Iranian J Sci Tech* 2010; **34**: 15-34.
38. Kaveh A, Talatahari S. Hybrid charged system search and particle swarm optimization for engineering design problems, *Eng Comput* 2011; 28 (4): 423-40.